Available online at www.sciencedirect.com
SCIENCE @ DIRECT®
Thin Solid Films 453–454 (2004) 150–153
thin solid films
www.elsevier.com/locate/tsf

(1 1 0)Nd:KGW waveguide films grown on CeO_2/Si substrates by pulsed laser deposition

P.A. Atanasov[a,b,*], T. Okato[a], R.I. Tomov[b], M. Obara[a]

[a]*Department of Electronics and Electrical Engineering, Keio University, 3-14-1, Hiyoshi, Kohoku-ku, Yokohama-shi 223-8522, Japan*
[b]*Institute of Electronics, Bulgarian Academy of Sciences, 72 Tsarigradsko Shose Boulevard, Sofia 1784, Bulgaria*

Abstract

Textured (1 1 0)Nd:KGW optical waveguides are grown on CeO_2/Si substrates by pulsed laser deposition. Ceria buffer layer is prepared on (1 0 0)Si substrates by KrF excimer laser ablation of $Ce_{0.9}Gd_{0.1}O_2$ ceramic target. The (1 0 0) or (1 1 1) orientation of CeO_2 depends on the deposition conditions. The Nd:KGW films are prepared by ablation of K-rich ceramic targets in O_2 or Ar. The influence of the synthesis conditions (O_2 or Ar pressure and substrate temperature) and the orientation of the CeO_2 buffer layer on the crystallinity of the Nd:KGW films are studied. Better results are obtained when deposited on (1 0 0)CeO_2/(1 0 0)Si. The as-grown films are optically active. The crystallinity improves and the intensity of the emission spectra increases upon annealing at 700 °C in air. The emission spectra of Nd:KGW films are demonstrated for the main Nd transitions in 0.85–1.45 μm spectral range. Waveguide loss as low as 3.3 dB cm^{-1} is measured.

PACS: 81.15.Fg; 42.70.Hj

Keywords: Pulsed laser deposition; Nd-doped potassium gadolinium tungstate; Ceria buffer layer; Structural and optical properties; Ceramic target

1. Introduction

In the last few years, increasing attention has been paid to the preparation of passive and active waveguides that are of great interest as components for integrated optics and optoelectronics. Among the materials with high potential for light generation or amplification, potassium gadolinium tungstate [$KGd(WO_4)_2$ or KGW] doped with rare-earth ions such as Nd, Er or Yb is of special interest [1–6]. Nd:KGW operates both in c.w. and Q-switched modes, provides an excellent match for diode pumping [6,7], has lower threshold and more than a factor of 2 higher slope efficiency than Nd:YAG lasers [2,8]. Moreover, it offers very efficient and ultra-low-threshold stimulated Raman scattering and thus allows simultaneous generation of the common Nd lines at 1.06, 1.35 and 0.89 μm together with several Stokes and Anti-Stokes lines [9,10]. Frequency doubling and mixing provides laser emission at numerous wavelengths in the range from 500 to 700 nm.

Nd-doped YAG [11] and GGG [12] optical thin films and active waveguide were successfully grown by pulsed laser deposition. Recently, thin Nd:KGW films have been grown for the first time [13]. They were deposited on sapphire and exhibit photoluminescence (PL) at 1.068 μm. Although some progress has been made [14–18], the growth of high quality Nd:KGW film is still a challenge. Deposition of these active materials on Si substrates is highly desirable to build integrated devices. The aim of the present work is to demonstrate the feasibility of growth of Nd:KGW films with good luminescent and optical properties on Si using ceria (CeO_2) as buffer layer. CeO_2 is used widely as a buffer layer or optical coating [19–21]. We chose it because its lattice parameters match well with those of Si and its index of refraction is lower than Nd:KGW, allowing for waveguide propagation. The growth conditions have been varied in order to achieve the optimum structural and optical properties of both—buffer and Nd:KGW thin films.

*Corresponding author. Tel.: +359-2-714-4382; fax: +359-2-975-3201.
E-mail address: paatanas@ie.bas.bg (P.A. Atanasov).

0040-6090/04/$ - see front matter © 2003 Elsevier B.V. All rights reserved.
doi:10.1016/j.tsf.2003.11.089

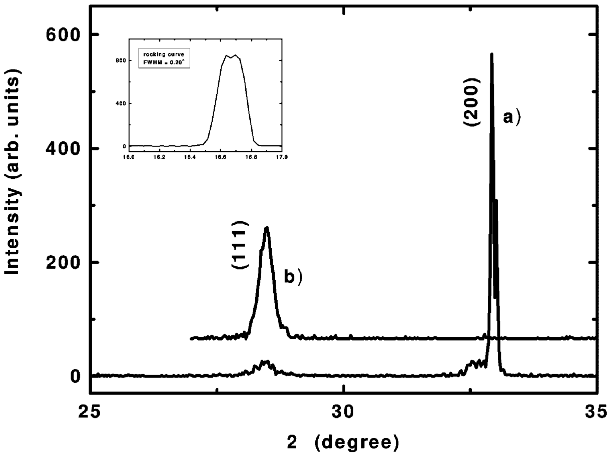

Fig. 1. XRD scan (curve a) and rocking curve (the insert) of (1 0 0)CeO_2 thin film: $E=4$ J cm^{-2}; $P(O_2)=0.012$ mbar; $T_s=500$ °C. XRD scan (curve b) of (1 1 1)CeO_2 of thin film: $E=4$ J cm^{-2}; $P(O_2)=0.025$ mbar; $T_s=500$ °C. The substrate is (1 0 0)Si.

2. Experimental

KrF excimer laser (COMPEX 200, Lambda Physik) operating at $\lambda=248$ nm, repetition rate $f=5$ Hz and $\tau=20$ ns is used for ablation of $Ce_{0.9}Gd_{0.1}O_2$ ceramic target. The optimum conditions for epitaxial growth obtained are: fluence $E=4$–5 J cm^{-2}; oxygen pressure $P(O_2)=0.012$–0.015 mbar; the target to substrate distance $d_{T-S}=50$ mm; and substrate temperature $T_s=$ 480–500 °C. The as-grown films are cooled down to the room temperature with a step of 50° min^{-1}.

KrF laser (LPX150, Lambda Physik), which operates at $f=20$ Hz and $\tau=27$ ns, is used for ablation of Nd:KGW ceramic targets. Target with $N_K/N_W=1.16$ (0.5 is the stoichiometric value) has been used, where N_K and N_W represent the number of K and W atoms, respectively. The Nd doping is evaluated to be approximately 1.2 at.%. The details for the target preparation are described in Ref. [17]. The laser fluence on the target is between 1.2 and 1.5 J cm^{-2} and $d_{T-S}=4$ cm. The substrate is heated from 650 to 750 °C. The pressure of Ar or O_2 is varied between 0.05 and 0.1 mbar. Usual deposition rate of ~8.5 nm min^{-1} is obtained. Some of the as-grown films are annealed at 700 °C in air.

The chemical composition is evaluated by EDX technique equipped with the environmental scanning electron microscope (XL-30 ESEM-FEG, Philips) and the crystallographic structure is determined by XRD equipment (RAD-C, Rigaku) used in the Bragg–Brentano configuration. The PL measurements are performed at room temperature using optical spectrum analyzer (Q8381A, ADVANTEST), where 810 nm line of fiber-coupled laser diode (OPC-A002-808-FC/150, OPTO POWER) is used for pumping. The surface morphology is observed using AFM (SPI3700, SEIKO). The waveguide loss is measured by recording the attenuation of the scattered light ($\lambda=633$ nm) along the propagation path. A rutile prism is used to couple the s-polarized He–Ne laser beam into the film. The light pattern is measured by a CCD camera. The incident angle of the laser light is determined to be 33.8°, having in mind that the refractive indexes at 633 nm of CeO_2 and KGW films are 1.68 and 1.90 [9], respectively. Finally, Raman scattering is measured by means of Raman spectroscopy (Raman One CCD, CHROMEX) using c.w. SHG Nd:YLF.

3. Results and discussions

3.1. CeO_2 growth on (1 0 0)Si substrate

Growth of (1 0 0)CeO_2 crystalline phase is very sensitive to the deposition conditions—T_s, $P(O_2)$ and E [22,23]. Moreover, it depends strongly on the quality of the amorphous SiO_2 layer formed on the silicon substrate. Beyond the exact optimum growth conditions obtained, a preferential (1 1 1)CeO_2 is formed. Cooling down of the as-deposited films is also important to prevent cracking. Additionally, a small amount of Gd is added (~3.3 at.%) to the target to prevent cracking (the thermal expansion of Si is two times lower than that of CeO_2) of the films having higher than 50 nm thickness. The thickness of the ceria layers is between 150 and 200 nm. XRD scans of typical texture (1 0 0) or (1 1 1)CeO_2 buffer layers are presented in Fig. 1 together with the (1 0 0)CeO_2 rocking curve. The typical value of $\Delta\omega=0.20°$ at FWHM for (1 0 0)CeO_2 suggests that the film has good crystallinity. The films have good morphology as seen from the AFM image—Fig. 2. The RMS surface roughness measured is less than 1 nm.

3.2. Nd:KGW films deposition

The potassium content in the Nd:KGW films strongly depends on the oxygen or Ar pressure [13–17]. It is

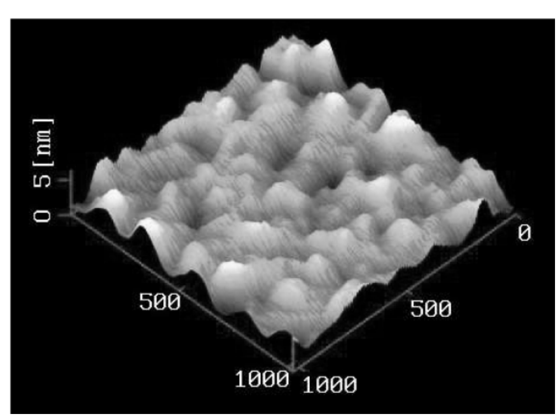

Fig. 2. AFM image of (1 0 0)CeO_2 thin film deposited on (1 0 0)Si.

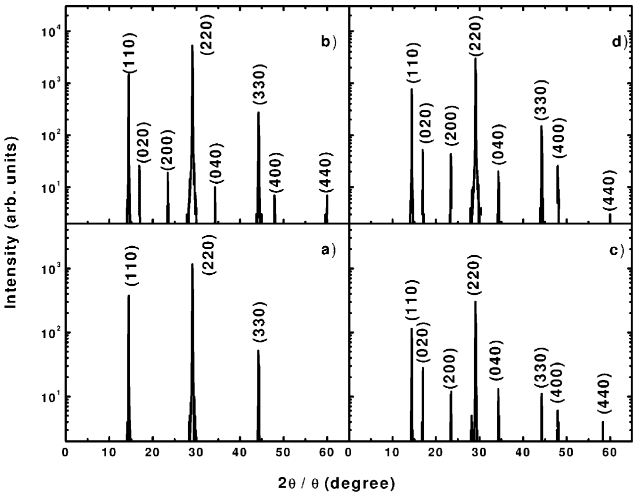

Fig. 3. XRD scans of films, deposited at $T_s = 700$ °C on (1 0 0)CeO_2/(1 0 0)Si: (a) $P(Ar) = 0.05$ mbar, (b) $P(Ar) = 0.08$ mbar; and (1 1 1)CeO_2/(1 0 0)Si: (c) $P(Ar) = 0.05$ mbar and (d) $P(Ar) = 0.08$ mbar.

very low for the films grown in vacuum ($< 10^{-4}$ mbar), increases with the ambient pressure, and becomes closer to the stoichiometric value ($N_K/N_W = 0.5$) in the range of optimum pressure achieved (0.05–0.08 mbar). The Nd, Gd and W contents are preserved for the deposition conditions applied. The O content is evaluated to be almost the same in the films grown in Ar or O_2. However, the films grown in Ar are slightly colored, which suggests the existence of some oxygen vacancy phase.

XRD spectra are very sensitive on the substrate temperature and ambient pressure. The optimum conditions with respect to the best crystal structure are: $T_s = 700$ °C and $P(Ar)$ or $P(O_2) = 0.08$ mbar. Pure (1 1 0)Nd:KGW crystalline phase is evident when deposited on (1 0 0)CeO_2—Fig. 3a and b. Using the rocking curves measured of the films deposited in both oxygen and Ar at optimum growth conditions, values of $\Delta\omega = 0.05°$ at FWHM are evaluated [18]. Same optimum growth conditions are obtained when deposited on (1 1 1)CeO_2/(1 0 0)Si. However, the crystallinity is worse—Fig. 3c and d. Some very shallow peaks of other Nd:KGW phases exist. In both cases, the crystal structure improves significantly, i.e. intensity of the peaks in the spectra increases and $\Delta\omega$ at FWHM decreases by factor of 2, after annealing in air at the temperature as high as 700 °C. This is more pronounced in case of films grown in Ar, which can be understood by compensation of oxygen vacancy.

The PL intensity is related to the crystallinity of the films. This is confirmed by PL spectra of the films deposited on both ceria orientations, i.e. films on (1 0 0) orientation have higher intensity compared to the (1 1 1) one—Fig. 4. However, the spectral structures are identical, similar to the Nd:KGW single crystal, but have two orders of magnitude lower intensity due to the smaller volume. In addition, it is worth pointing out that the ratio of emission intensity of the $^4F_{3/2} \rightarrow {}^4I_{11/2}$ band (main transition at 1067 nm) to that of $^4F_{3/2} \rightarrow {}^4I_{9/2}$ band (911 nm), which is less than two for the single crystal, is smaller for the thin films. In fact, it is near one in the case of the films grown in O_2 (Fig. 4b). Therefore, these films are well suitable for lasing at $^4F_{3/2} \rightarrow {}^4I_{9/2}$ band, reaching a quantum efficiency of 0.89. This is an interesting additional result, which will require further investigations. Annealing at the growth temperature significantly improves the crystallinity of the films and thus PL intensity increases by factor of 2—Fig. 5.

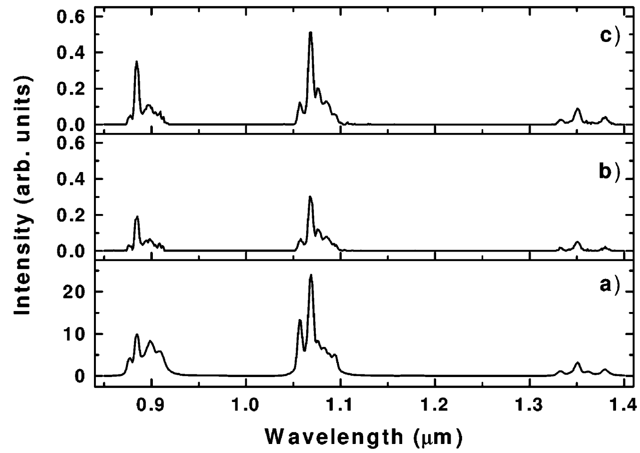

Fig. 4. Nd:KGW fluorescence spectra over 850–1450 nm: (a) single crystal; (b) thin film on (1 1 1)CeO_2/(1 0 0)Si; (c) thin film on (1 0 0)CeO_2/(1 0 0)Si. $P(Ar) = 0.08$ mbar, $T_s = 700$ °C.

The RMS surface roughness values of Nd:KGW films measured are approximately 70 nm when deposited in O_2 and exceed 150 nm in Ar. Generally, the optical

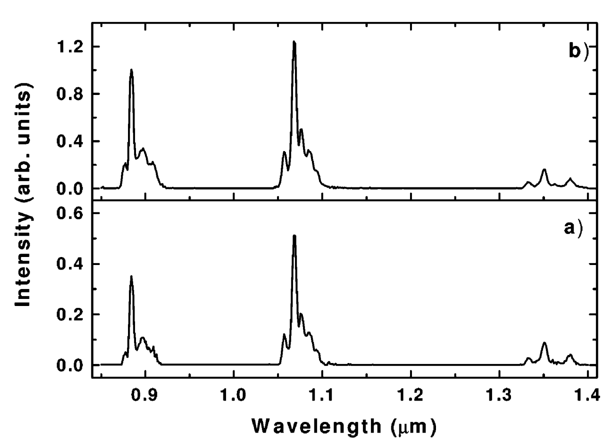

Fig. 5. Nd:KGW fluorescence spectra over 850–1450 nm: (a) as-deposited film; (b) annealed at 700 °C for 1 h in air. Substrate (1 0 0)CeO_2/(1 0 0)Si, $P(Ar) = 0.08$ mbar, $T_s = 700$ °C.

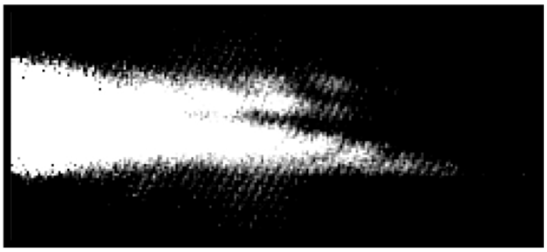

Fig. 6. CCD image of the waveguide propagation in Nd:KGW film grown in Ar.

properties of the films are better when using O_2, although the crystallinity is better in case of Ar. The most transparent film is obtained at the optimum conditions mentioned above: $P(O_2)=0.08$ mbar and $T_s=$ 700 °C. In this case, the optical waveguide loss of film deposited on (1 0 0)CeO_2/(1 0 0)Si is evaluated to be approximately 3.3 dB cm^{-1} at 633 nm. Fig. 6 shows CCD image of waveguide propagation of the film deposited at $P(Ar)=0.08$ mbar and $T_s=700$ °C. As it is seen, the image is split at the end of its propagation. This is probably a result of the anisotropy of (1 1 0)Nd:KGW films.

The Raman spectra are also related to the crystallinity and the highest intensity of the Nd:KGW peaks at 768.8 and 903 cm^{-1} corresponds to the best quality films deposited at the optimum growth conditions in Ar. However, the peaks are slightly (several cm^{-1}) shifted with respect to those of the single crystal and their widths (at FWHM) are approximately twice as broad. This is crystal distortion caused by the lattice mismatch between the Nd:KGW films and the substrate.

4. Conclusions

Textured (1 1 0)KGW thin films are successfully grown on (1 0 0)Si substrate by introducing (1 0 0) or (1 1 1)CeO_2 buffer layer. The potassium deficiency in the films is compensated by use of K-rich ceramic target. The contents of Nd, Gd and W are preserved as the stoichiometric values. The O content of the films grown in Ar or O_2 is unchanged within the dispersion errors when determined via EDX. The film crystallinity and PL intensity are better when deposited in Ar ambient than O_2. However, the as-grown films' color and the annealing effects suggest that there is oxygen vacancy in the films grown in Ar. They have rougher surface morphology and anisotropy. The optimum growing conditions obtained from the point of crystallinity, optical properties and surface morphology are: $P(O_2)=0.08$ mbar, $T_s=700$ °C and (1 0 0)CeO_2/(1 0 0)Si substrate. In this case, the optical waveguide loss is evaluated to be 3.3 dB cm^{-1}. The emission intensity of the $^4F_{3/2} \rightarrow {}^4I_{9/2}$ band (911 nm) has larger relative value compared to this of the single crystal.

Acknowledgments

The work was supported in part by EU project NANOPHOS, Contract IST-2001-39112 and Project No. F-1104/01 with BNSF, Bulgaria. P.A. Atanasov acknowledges the JSPS, Japan for financial support.

References

[1] A.A. Kaminskii, P.V. Klevtsov, A.A. Pavlyuk, Phys. Stat. Solidi A 5 (1971) K79.
[2] V. Kushawaha, A. Banerjee, L. Major, Appl. Phys. B 56 (1993) 239.
[3] I.V. Mochalov, Opt. Eng. 36 (1995) 1660.
[4] N.V. Kuleshov, A.A. Lagatsky, V.G. Shcherbitsky, V.P. Mikhailov, E. Heumann, T. Jensen, A. Diening, G. Huber, Appl. Phys. B 64 (1997) 409.
[5] A.A. Lagatsky, N.V. Kuleshov, V.P. Mikhailov, Opt. Commun. 165 (1999) 71.
[6] M.C. Pujol, M. Rico, C. Zaldo, R. Solé, V. Nikolov, X. Solans, M. Aguiló, F. Díaz, Appl. Phys. B 68 (1999) 187.
[7] T. Graf, J.E. Balmer, Opt. Eng. 34 (1995) 2349.
[8] O. Musset, J.P. Boquillon, Appl. Phys. B 64 (1997) 503.
[9] V. Kushawaha, Y. Yan, Y. Chen, Appl. Phys. B 62 (1996) 533.
[10] A.A. Demidovich, A.N. Kuzmin, G.I. Ryabtsev, W. Strek, A.N. Titov, Spectrochim. Acta A 54 (1998) 1711.
[11] M. Ezaki, H. Kumagai, K. Kobayashi, K. Toyoda, M. Obara, Jap. J. Appl. Phys. 1 (34) (1995) 6838.
[12] D.S. Gill, A.A. Anderson, R.W. Eason, T.J. Warburton, D.P. Shepherd, Appl. Phys. Lett. 69 (1996) 10.
[13] P.A. Atanasov, R.I. Tomov, J. Perriére, R.W. Eason, N. Vainos, A. Klini, A. Zherikhin, E. Millon, Appl. Phys. Lett. 76 (2000) 2490.
[14] P.A. Atanasov, M. Jiménez de Castro, A. Perea, J. Perriére, J. Gonzalo, C.N. Afonso, Appl. Surf. Sci. 186 (2002) 469.
[15] P.A. Atanasov, A. Perea, M. Jiménez de Castro, J.A. Chaos, J. Gonzalo, C.N. Afonso, J. Perriére, Appl. Phys. A 74 (2002) 109.
[16] M. Jelínek, J. Lancok, M. Pavelka, P.A. Atanasov, A. Macková, F. Flory, C. Garapon, Appl. Phys. A 74 (2002) 481.
[17] T. Okato, P.A. Atanasov, M. Obara, Appl. Phys. A 77 (2003) 395.
[18] T. Okato, P.A. Atanasov, R.I. Tomov, M. Obara, Appl. Phys. A 77 (2003) 775.
[19] A. Hartridge, M. Ghanashyam Krishna, A.K. Bhattacharya, Int. J. Modern Phys. B 12 (1998) 1573.
[20] A. Wang, J.A. Belot, T.J. Marks, P.R. Markworth, R.P.H. Chang, M.P. Chudzik, C.R. Kannewurf, Physica C 320 (1999) 154.
[21] C.H. Chen, T. Koguchi, A. Saiki, N. Wakiya, K. Shinozaki, N. Mizutani, Appl. Phys. A 76 (2002) 969.
[22] M.W. Denhoff, J.P. McCaffrey, J. Appl. Phys. 70 (1991) 3986.
[23] X.D. Wu, R.C. Dye, R.E. Muenchansen, S.R. Foltyn, M. Maley, A.D. Rollett, A.R. Garcia, N.S. Nogar, Appl. Phys. Lett. 58 (1991) 2165.